

A QUADRIC SURFACE MODEL OF VACUUM TUBES FOR VIRTUAL ANALOG APPLICATIONS

Riccardo Giampiccolo

DEIB, Politecnico di Milano
Milan, Italy
riccardo.giampiccolo@polimi.it

Stefano D'Angelo

Orastron Srl
Sessa Cilento, Italy
stefano.dangelo@orastron.com

Alberto Bernardini

DEIB, Politecnico di Milano
Milan, Italy
alberto.bernardini@polimi.it

Augusto Sarti

DEIB, Politecnico di Milano
Milan, Italy
augusto.sarti@polimi.it

ABSTRACT

Despite the prevalence of modern audio technology, vacuum tube amplifiers continue to play a vital role in the music industry. For this reason, over the years, many different digital techniques have been introduced for accomplishing their emulation. In this paper, we propose a novel quadric surface model for tube simulations able to overcome the Cardarilli model in terms of efficiency whilst retaining comparable accuracy when grid current is negligible. After showing the model capability to well outline tubes starting from measurement data, we perform an efficiency comparison by implementing the considered tube models as nonlinear 3-port elements in the Wave Digital domain. We do this by taking into account the typical common-cathode gain stage employed in vacuum tube guitar amplifiers. The proposed model turns out to be characterized by a speedup of $4.6\times$ with respect to the Cardarilli model, proving thus to be promising for real-time Virtual Analog applications.

1. INTRODUCTION

Vintage audio gear based on tube amplifiers is known for producing many of the distinctive sounds that characterize music genres such as blues, rock, and metal. Many professional electric guitar players prefer tube amplifiers due to the pleasing distortion they produce, resulting in a rich and warm sound. However, the high cost of reproducing tube-based analog audio gear and the decreasing supply of electrical components used in popular pieces of audio equipment have made these sounds inaccessible to many. As a result, Virtual Analog (VA) modeling has become a popular alternative as it seeks to create digital algorithms that accurately replicate the behavior of analog audio effects. This has resulted in many software implementations that serve as convenient digital counterparts for expensive, bulky, and fragile analog equipment, of which tube guitar amplifiers are a noteworthy example.

Two broad categories of models are used in VA modeling: “black-box” models that emulate the effect of a specific piece of gear by replicating its input-output behavior, using, for example,

neural networks [1], Volterra series [2], or block-oriented Wiener-Hammerstein models [3]; “white-box” methods which emulate the reference circuit by solving the corresponding system of ordinary differential equations (or differential algebraic equations), using, for example, the Port-Hamiltonian approach [4], the State-space approach [5], or Wave Digital Filters (WDFs) [6, 7]. In this work, we are interested in deriving efficient “white-box” models of audio circuits with vacuum tubes, such that we can leverage the knowledge of schematics in order to address VA modeling.

Among vacuum tubes, triodes are the most widespread [8]. Before the advent of solid-state electronics, these devices were used in a variety of audio circuits, including preamplifiers, power amplifiers, equalizers, and compressors. In particular, the basic construction of a triode vacuum tube consists of three main components [9]: a cathode, a grid, and an anode (also known as plate). The cathode is a heated filament that emits electrons, while the anode is a positively charged electrode that attracts the electrons. The grid is a wire mesh located between the cathode and the anode that can control the flow of electrons between them. Over the years, many other designs of vacuum tubes have been introduced, mostly adding other grids between cathode and plate (e.g., pentodes).

Several models of vacuum tubes have been presented so far [8, 10]. In [11], tubes are modeled by combining linear filters and waveshapers, while the state-space approach and numerical methods are used in [12] and [13], respectively. Nonetheless, numerous implementations make use of WDFs. In fact, in the WD domain, circuits with up to one nonlinear element described by an explicit mapping can be solved with no use of iterative solvers, even using stable discretization methods (e.g., Backward Euler, trapezoidal rule, etc.), making WDFs interesting for real-time scenarios [14]. For instance, examples of WDF tube implementations can be found in [15], [16], [17], [18], [19], or [20], in which triodes are modeled combining Wave Digital (WD) principles to neural networks. However, most of the implementations available in the literature refer to two triode models: Koren [21] and Cardarilli models [22]. The first is based on a phenomenological model of the triode operation, while the second provides a simple yet accurate representation of triodes using a set of analytical expressions that describe the tube transfer function.

In this paper, we propose a new quadric surface model of vacuum tubes which is characterized, at the same time, by high efficiency and accuracy as long as grid current is negligible. Starting

Copyright: © 2023 Riccardo Giampiccolo et al. This is an open-access article distributed under the terms of the Creative Commons Attribution 4.0 International License, which permits unrestricted use, distribution, adaptation, and reproduction in any medium, provided the original author and source are credited.

from the generic equation describing quadric surfaces and considering a grid current equal to zero, we obtain a multivariate quadric equation able to outline the plate-to-cathode characteristics of triodes in active region employing just three parameters. These can be then fitted on datasheet or measurement data by applying a simple least squares method [23]. With respect to Koren model, the proposed approach is more accurate and almost as accurate as Cardarilli model if we assume a null grid current. Moreover, the model is characterized by a lower number of parameters, making the fitting operation more lightweight and simple. Although many different implementations of the proposed model can be pursued, we decided to realize it as a 3-port Wave Digital (WD) block, which we later employed for emulating the common-cathode gain stage typically found in tube guitar amplifiers.

The paper is organized as follows. In Section 2, we provide a background on triode modeling, by discussing both Koren and Cardarilli models. We introduce the proposed quadric surface model in Section 3, and we draw a first comparison with the traditional models presented in the previous section focusing on their accuracy. Then, in Section 4, we address the emulation of a typical common-cathode gain stage considering the famous 12AX7 triode, and we run a comparison with Cardarilli model regarding the efficiency. Section 5 concludes this paper.

2. BACKGROUND ON TRIODE MODELING

Let us consider the vacuum tube depicted in Fig. 1(a). Such a device presents three terminals, and thus, it is typically known under the name of *triode*. The basic structure of a triode consists of an evacuated glass envelope containing three electrodes: a *cathode* “k” (or heated filament), a *grid* “g”, and a *plate* “p” (also referred to as anode). Such a vacuum tube is the ancestor of modern transistors; in fact, it functions as an electronic amplifier by controlling the flow of electrons between the cathode and anode via the electric field generated by the grid [10]. By modulating the voltage applied to the grid, the current flow between the cathode and anode can be varied, allowing for amplification of signals. A triode operates as a “normally on” device, meaning that electrons flow to the positively biased plate even when the grid voltage is at its quiescent value. As the grid becomes more negative with respect to the cathode, the anode current is progressively reduced. Hence, in order to prevent the anode current to be turned off, a constant voltage is typically applied to the cathode. Moreover, the bias ensures that the positive peaks of the signal do not drive the grid voltage close to the cathode one, which would result in nonlinear behavior and the generation of grid current. The grid voltage that completely blocks electrons from reaching the anode is, instead, called *cutoff voltage*. Finally, in order to obtain linear amplification, the voltage on the grid must remain above the cutoff voltage without exceeding the cathode potential.

Different models of triodes are available in the literature. Usually, such models rely on a current source for the plate current i_p that is dependent on both the grid-to-cathode voltage V_{gk} and the plate-to-cathode voltage V_{pk} [9]. In the following, we present two traditional models widely used for VA applications, i.e., Koren [21] and Cardarilli [22] models.

2.1. Koren Model

In [21], Koren presents a phenomenological model able to describe the behavior of triodes making use of a small amount of param-

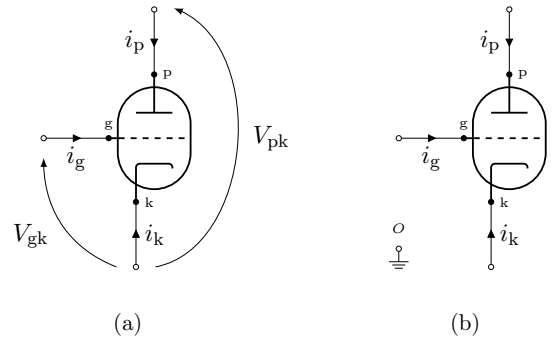


Figure 1: (a) Circuit symbol of the triode reporting the current and voltage conventions employed in this paper. The plate is marked with “p”, the grid is marked with “g”, while the cathode is marked with “k.” (b) Triode augmented with the reference node O.

Table 1: Parameters for modeling 12AX7 triode with Koren model [21].

Parameter	Value	Parameter	Value
k	1.4	k_{g1}	1060 V ^k /A
k_k	600	μ_k	100
k_{vb}	300 V ²	—	—

ters. The model equations are designed such that the plate current $i_p > 0$ whenever the plate-to-cathode voltage $V_{pk} > 0$. In particular, Koren model is defined as follows

$$i_p = \frac{V_1^k}{k_{g1}} (1 + \text{sgn}(V_1)) , \quad (1)$$

$$i_k = -i_p - i_g , \quad (2)$$

where i_k and i_g are the cathode and grid currents, respectively, and

$$V_1 = \frac{V_{pk}}{k_k} \log \left(1 + \exp \left(k_k \left(\frac{1}{\mu_k} + \frac{V_{gk}}{\sqrt{k_{vb} + V_{pk}^2}} \right) \right) \right) , \quad (3)$$

$$V_{gk} = V_g - V_k , \quad V_{pk} = V_p - V_k ,$$

whereas $\text{sgn}(\cdot)$ is the sign function, μ_k is the amplification factor, and k , k_{g1} , k_k , and k_{vb} are real parameters. Moreover, V_p , V_g , and V_k are the plate, grid, and cathode voltages, respectively. Koren already provides the values of such parameters for modeling the main triodes found in audio circuitry [21], as well as fitting methodologies for obtaining implementations of custom triodes. The positive direction of tube currents and voltages are assumed to be compliant with Fig 1(a). Furthermore, Koren model entails a diode between grid and cathode; as a matter of fact, i_g is typically computed employing common diode models or approximated with a time-varying resistor dependent on the grid-to-cathode voltage, as explained in [24]. Finally, it is worth pointing out that such a model is derived assuming that plate and grid are mutually insulated [21].

Table 2: Parameters for modeling 12AX7 triode with Cardarilli model [22].

Parameter	Value	Parameter	Value
G_0	1.102 mA/V ^{2/3}	μ_0	99.705
G_1	15.12 μ A/V ^{5/3}	μ_1	-22.98 kV ⁻¹
G_2	-31.56 μ A/V ^{8/3}	μ_2	-0.4489 V ⁻²
G_3	-3.286 μ A/V ^{11/3}	μ_3	-22.27 kV ⁻³
h_0	0.6 V	V_{off}	-0.2 V
h_1	0	D	0.12
h_2	0 V ⁻¹	K	1.1
h_3	0 V ⁻²	-	-

2.2. Cardarilli Model

The triode model developed by Cardarilli *et al.* [22] relies on a unique approach that combines physical and interpolative techniques. This model replaces the constant parameters typically used in classical formulations for plate current i_p and grid current i_g with splines that depend on the grid-to-cathode voltage V_{gk} . The resulting model, which is based on the current and voltage directions illustrated in Fig. 1(a), is defined as

$$i_p = G \sqrt{\left(V_{gk} + \frac{V_{pk}}{\mu} + h \right)^3}, \quad (4)$$

$$i_g = \begin{cases} \frac{i_p}{1+D \left(\frac{V_{pk}}{V_{gk}-V_{\text{off}}} \right)^K} & \text{if } V_{gk} > V_{\text{off}} \\ 0 & \text{if } V_{gk} \leq V_{\text{off}} \end{cases}, \quad (5)$$

$$i_k = -i_p - i_g, \quad (6)$$

where

$$G = \sum_{i=0}^3 G_i V_{gk}^i, \quad \mu = \sum_{i=0}^3 \mu_i V_{gk}^i, \quad h = \sum_{i=0}^3 h_i V_{gk}^i, \quad (7)$$

and G is the perveance, μ is the amplification factor, h models the effects introduced by the initial electron velocity, while V_{off} is the threshold grid-to-cathode voltage above which grid current is present. The classical plate-current formulation shown in (4) plays a significant role in describing the behavior of triodes. In addition, for the case $V_{gk} > V_{\text{off}}$, the grid current expression of (5) is similar to the empirical relation presented in [9], where the numerical constants K and D help taking into account the contact potential effect.

Together, these formulas offer a valuable insight into the functioning of triodes and are useful tools for analyzing and modeling their behavior in electronic circuits. Moreover, in [22] a technique for calculating the values for all the parameters shown in (4), (5), and (7) based on curve fitting of datasheet data is presented. This approach helps to ensure the accuracy of the model, which has been shown to reproduce the transconductance behavior of triodes with high fidelity. Finally, unlike other triode models, Cardarilli model can provide highly accurate results even in saturation conditions.

Table 3: Parameters for modeling 12AX7 triode with the proposed model.

Parameter	Value	Parameter	Value
k_p	1.014×10^{-5}	k_{pg}	1.076×10^{-5}
k_{p2}	$5.498 \times 10^{-8} \text{ V}^2$	-	-

3. PROPOSED QUADRIC SURFACE MODEL

In this section, we propose a new memoryless triode model based on a quadric surface approximation. The model is characterized by a lower number of parameters and by simpler mathematical operations with respect to those involved in the two traditional models of Section 2. On the other hand, for the sake of computational efficiency, it assumes null grid current, thus sacrificing accuracy when the grid voltage approaches and exceeds the cathode voltage.

The model is derived by exploiting the similarity between part of the typical triode characteristics $i_p(V_{gk}, V_{pk})$ and a quadric surface. In particular, we start by considering the general quadric surface equation [26]

$$k_{p2} V_{pk}^2 + k_{g2} V_{gk}^2 + k_2 i_p^2 + k_{pg} V_{gk} V_{pk} + k_{pk} V_{pk} i_p + k_{gk} V_{gk} i_p + k_p V_{pk} + k_g V_{gk} + k_1 i_p + k_0 = 0, \quad (8)$$

where k_{p2} , k_{g2} , k_2 , k_{pg} , k_{pk} , k_{gk} , k_p , k_g , k_1 , k_0 are real coefficients. In order to exploit such an equation for modeling the plate current i_p , we set $k_1 = -1$ and $k_2 = k_{pk} = k_{gk} = 0$ for avoiding dependences on i_p cross-products or second-order powers, yielding

$$i_p = k_{p2} V_{pk}^2 + k_{g2} V_{gk}^2 + k_{pg} V_{gk} V_{pk} + k_p V_{pk} + k_g V_{gk} + k_0. \quad (9)$$

It is worth pointing out that in (9), the terms V_{gk} and V_{pk} are present with all the powers up to the second order, allowing us to account for different contributions of both the plate-to-cathode voltage and the grid-to-cathode voltage whilst increasing the descriptive capability of the model.

Looking at the typical triode characteristics in datasheets, we recognize that the different curves obtained by varying V_{gk} are somehow tangent to the V_{pk} -axis in the $i_p - V_{pk}$ plane. Therefore, by imposing $i_p = 0$ and solving for V_{pk} , we obtain

$$V_{pk} = \frac{\sqrt{\Delta} - V_{gk} k_{pg} - k_p}{2k_{p2}} \quad (10)$$

with

$$\Delta = V_{gk}^2 (k_{pg}^2 - 4k_{g2} k_{p2}) + V_{gk} (2k_p k_{pg} - 4k_g k_{p2}) - 4k_0 k_{p2} + k_p^2, \quad (11)$$

and, by enforcing $\Delta = 0$, we constraint the vertex of the quadric to be on the V_{pk} -axis. If we then solve it for k_0 , we obtain

$$k_0 = \frac{V_{gk}^2 (k_{pg}^2 - 4k_{g2} k_{p2}) + V_{gk} (2k_p k_{pg} - 4k_g k_{p2}) + k_p^2}{4k_{p2}}, \quad (12)$$

which once substituted into (9) yields

$$\begin{aligned} i_p &= k_{p2} V_{pk}^2 + \frac{k_{pg}^2}{4k_{p2}} V_{gk}^2 + k_{pg} V_{gk} V_{pk} + k_p V_{pk} + \frac{k_p k_{pg}}{2k_{p2}} V_{gk} + \frac{k_p^2}{4k_{p2}} \\ &= i_p(V_{pk}) = i_{pk}. \end{aligned} \quad (13)$$

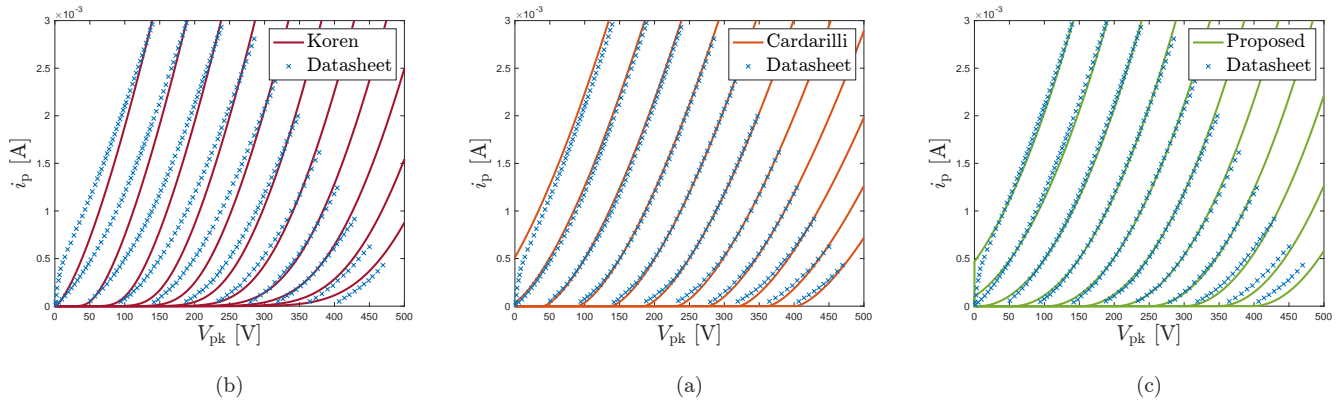


Figure 2: Accuracy comparison between the $i_p - V_{pk}$ characteristics obtained with Koren model (a), Cardarilli model (b), and proposed model (c) and the one reported on the 12AX7 datasheet [25].

For any given V_{gk} , (13) describes a parabola whose vertex lies on the V_{pk} -axis. In order to match datasheet curves [25], we only use the branch where the first derivative of i_p with respect to V_{pk} , i.e.,

$$i'_p = \frac{di_p(V_{pk})}{dV_{pk}}, \quad (14)$$

is non-negative, and assume i_p to be equal to zero otherwise. Therefore, considering once again the conventions reported in Fig. 1(a) and the initial hypothesis on the grid current, we may write down the proposed quadric surface model as follows

$$i_p = \begin{cases} i_{pk} & i'_p \geq 0 \\ 0 & i'_p < 0 \end{cases}, \quad (15)$$

$$i_g = 0, \quad (16)$$

$$i_k = -i_p - i_g. \quad (17)$$

In any case, $V_{pk} \geq 0$ is also always assumed to hold true, as otherwise a region with negative static resistance would be introduced.

It is worth pointing out that the real coefficients of (13) can be computed starting from datasheets or measurements data, making use of common fitting techniques, such as a simple least squares method [23]. Moreover, as anticipated at the beginning of the section, the model presents just three parameters, which do increase the convergence performance of such fitting techniques, making it suitable to model with ease triodes available on the market. Then, the model mainly relies on a second-order formula which leads to closed-form solutions when equated to similar simple expressions (e.g., when coupled with linear systems), which makes it particularly suited for implementing fully-explicit white-box circuit models when such conditions are met. Finally, the quadric surface model is also able to describe pentodes in triode configuration.

In order to test the accuracy of the representation, we compare the $i_p - V_{pk}$ characteristics found on datasheets to that obtained by means of the proposed model. We do this also for the two traditional models presented in Section 2. Let us take into account the famous 12AX7 triode, which was employed in many different tube stages, as our reference vacuum tube. Tables 1, 2, 3 report the values of the coefficients to be used for modeling such a triode with Koren model, Cardarilli model, and proposed model, respectively. Fig. 2, instead, reports the results of such a comparison;

the 11 curves present in each of the three plots are obtained by considering different values of V_{gk} . From the leftmost up to the rightmost, these curves are computed with V_{gk} equal to 0, -0.5 , -1 , -1.5 , -2 , -2.5 , -3 , -3.5 , -4 , -4.5 , -5 . In particular, in Fig. 2(a) the results of Koren model are reported, in Fig. 2(b) those of Cardarilli model, while in Fig. 2(c) those of the quadric surface model. In all the three plots, the data acquired from the 12AX7 datasheet [25] are marked with blue crosses. In Fig. 2, it is possible to observe that, in common operating regions [27], the proposed model is more accurate than Koren model and is almost as accurate as Cardarilli model, while featuring a lower number of parameters. In fact, the 15 parameters controlling Cardarilli model allows this to better grasp the nuances at higher V_{pk} . Nonetheless, we can state that the proposed model maintain, in general, a comparable accuracy since the of values of V_{pk} for which it starts to deviate from the measured characteristics are not often encountered in real applications.

3.1. 3-port Wave Digital Implementation

Although the proposed model can be implemented making use of different techniques, in this work we decided to use WDFs. The design procedure of WDFs entails a port-wise description of the reference circuit, whose elements and topological interconnections are realized as input-output blocks characterized by scattering relations. In order to accomplish such a description, WDFs make use of a change of variable, turning port voltage v and port current i (the so-called Kirchhoff variables) into incident wave a and reflected wave b with the addition of a free parameter per port Z called *port resistance* [6]. Such a free parameter constitutes a powerful mean for removing delay-free loops formed when Wave Digital (WD) blocks are interconnected [6, 28]. Among the different wave definitions present in the literature [6, 29, 30], the most widespread is that of voltage waves, i.e.,

$$\begin{aligned} a &= v + Zi, & b &= v - Zi, \\ v &= \frac{a+b}{2}, & i &= \frac{a-b}{2Z}, \end{aligned} \quad (18)$$

which is employed for deriving WD implementations of circuit elements [7, 31] and N -port topological junctions [32]. We aim at deriving a triode WD implementation of the quadric surface model

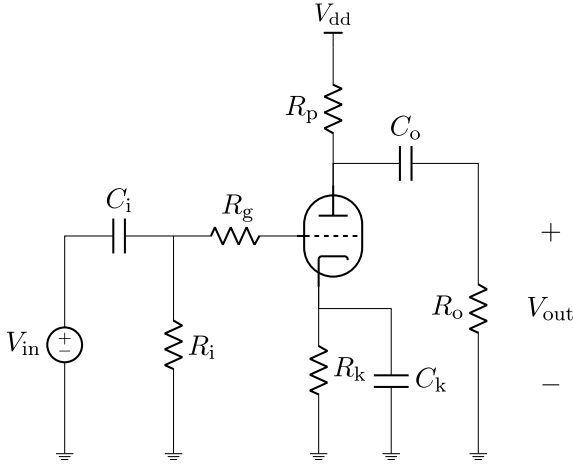


Figure 3: Typical common-cathode gain stage found in tube amplifiers.

such that it can be used in common WD structures. In particular, we here derive a 3-port triode model following the approach described in [18, 33]. Hence, we add a reference node O to the triode model, as shown in Fig. 1(b), and name the port between the p node and O as port 1, the port between the g node and O as port 2, and the port between the k node and O as port 3. Such a reference node will be coincident with the ground node when the model is exploited for circuit emulation. Then, each of these ports is characterized by the set of variables $\{a_x, b_x, Z_x\}$ with $x = 1, 2, 3$ being the port number.

If we apply the linear transformation in (18) to (16) and (17), and solving for b_2 and b_3 we readily obtain

$$b_2 = a_2, \quad (19)$$

$$b_3 = a_3 + \frac{Z_3}{Z_1}(a_1 - b_1), \quad (20)$$

while doing the same with (15) and solving for b_1 gives us

$$b_1 = \pm \frac{\sqrt{\Delta_1}}{\sqrt{2Z_1 k_{p2} \gamma}} - \frac{1}{4Z_1 k_{p2} \gamma^2} - \eta, \quad (21)$$

where

$$\Delta_1 = \frac{1}{8Z_1 k_{p2} \gamma^2} + a_1 + \eta, \quad (22)$$

$$\gamma = 1 + \frac{Z_3}{Z_1} \left(1 + \frac{k_{pg}}{4k_{p2}} \right), \quad (23)$$

$$\eta = \frac{\beta + \frac{\alpha}{2}}{k_{p2} \gamma}, \quad (24)$$

$$\alpha = k_p + k_{pg} \left(a_2 - a_3 - \frac{Z_3}{2Z_1} a_1 \right), \quad (25)$$

$$\beta = k_{p2} \left(\frac{1 - \frac{Z_3}{Z_1} a_1 - a_3}{2} \right). \quad (26)$$

Using the above equations, we can express

$$\begin{aligned} i'_p &= k_{pg} V_{gk} + 2k_{p2} V_{pk} + k_p = \\ &= k_{pg} \left(\frac{Z_3}{2Z_1} (b_1 - a_1) + a_2 - a_3 \right) + \\ &\quad + k_{p2} \left(\frac{Z_3}{Z_1} (b_1 - a_1) + b_1 + a_1 - 2a_3 \right) + k_p, \end{aligned} \quad (27)$$

and hence

$$i'_p \geq 0 \Leftrightarrow b_1 \geq -\eta, \quad (28)$$

assuming that all the involved model parameters and port resistances are positive. This should always be the case given how the model was constructed and that negative port resistances are related to incompatible sign conventions [34]. By comparing (28) with (21), it is evident that the first term in this last equation must be positive (necessary but not sufficient condition), hence the square root must be taken with the positive sign.

Since (21) is effectively the solution of the intersection of a line with a paraboloid pointing downwards in a 4-dimensional space, the cases in which $\Delta_1 < 0$, and thus in which such an intersection does not exist, can be interpreted as if V_{pk} or i_{pk} are too small or negative. In order to handle these occurrences, as well as the cases in which the resulting V_{pk} , i_{pk} , or i'_p are negative, we propose the following algorithm:

1. compute Δ_1 using (22);
2. if $\Delta_1 \geq 0$ then
 - (a) compute b_1 using (21) taking the square root with positive sign;
 - (b) if $i'_p < 0$, computed according to (27), force $i_p = 0$ (open circuit condition) by setting $b_1 = a_1$;
 otherwise, if $\Delta_1 < 0$ set $b_1 = a_1$ (i.e., $i_p = 0$, open circuit condition);
3. if the resulting $V_{pk} < 0$, force it to be $V_{pk} = 0$ by setting

$$b_1 = \frac{(Z_3 - Z_1)a_1 + 2Z_1 a_3}{Z_1 + Z_3} \quad (29)$$

according to (18) and (20).

Please notice that such a model is implemented in a fully explicit fashion, i.e., without the need for iterative solvers. Furthermore, it is worth pointing out that the quadric surface model can be also realized as a 2-port WD block, for example by employing the vector definition of waves in [30, 35], or, more generally, as a N -port with $N \leq 6$ following the approach discussed in [33]. Different WD implementations of the proposed model may lead to different advantages, potentially broadening the class of circuit models that can be implemented in an explicit fashion. For instance, the WD 2-port implementation by means of vector waves would allow us to explicitly realize triode stages with Miller capacitance or characterized by complicated topologies [9], which, instead, may not be realized by means of the 3-port implementation. However, when the number of multi-port nonlinear elements is ≥ 2 , iterative methods must be employed for the solution of the WD structure [31].

4. EXAMPLE OF APPLICATION

Let us consider the common-cathode gain stage shown in Fig. 3, typically found in tube amplifiers. The same circuit has been taken into account in many other publications concerning the emulation

Table 4: Values of the circuital components of Fig. 3.

Parameter	Value	Parameter	Value
V_{dd}	250 V	R_p	100 k Ω
R_i	1 M Ω	R_o	1 M Ω
R_g	20 k Ω	R_k	1 k Ω
C_k	10 μ F	C_i	100 nF
C_o	10 nF	—	—

of vacuum tubes, e.g., in [18]. With reference to the triode stage, the input signal is represented by the voltage generator V_{in} . Capacitor C_i and resistor R_i form a highpass filter which removes the DC (Direct-Current) component from the input if present. The cathode circuit, instead, is composed of a parallel connection between resistor R_k and capacitor C_k , and sets the signal-dependent biasing for the triode. The plate is connected to the DC voltage source V_{dd} via resistor R_p , which is responsible for the node “p” bias point. Then, the plate is also connected to the series between the DC decoupling capacitor C_o and load resistance R_o , whose voltage is taken as output variable. The values of the circuital parameters are reported in Table 4. The nonlinear amplification introduced by the triode together with the dynamic nature of the stage can generate a rather complex signal-dependent distortion on the output V_{out} .

We implement the common-cathode stage in the WD domain following the same approach and using the same WD structure employed in [18], i.e., by considering the 3-port WD block modeling the triode at the root of a connection tree. In order to test the accuracy of the WD implementation, we realize the same circuit in LTspice, which is a widespread freeware software for circuit simulations, together with the proposed triode model. We set $V_{in} = A \sin(2\pi k f_0 / f_s)$, where $A = 2.5$ V is the amplitude, k is the sampling index, $f_0 = 1$ kHz is the fundamental frequency, and $f_s = 44.1$ kHz is the sampling frequency; in addition, we consider the duration of the sinusoidal input equal to 1 s. We select once again the 12AX7 as our reference triode, whose model parameters are reported in Table 3. Fig 4 shows the output of the simulation, in particular the first three periods. The green dashed curve representing the LTspice simulation is overlapped with the continuous blue curve representing the WD simulation, pointing out the accuracy of the representation. Moreover, Fig. 4 also reports the results of the WD simulation obtained substituting the proposed triode model with the WD 3-port implementation of Cardarilli model (with no grid current) proposed in [18]. We select Cardarilli model over Koren model for drawing a comparison with state-of-the-art implementations of triodes since it is characterized by a higher accuracy, as shown in Fig. 2. Looking at Fig. 4, we can state that the two different realizations of the common-cathode stage are consistent, and that just a slightly different behavior can be spotted for the negative half-wave, which reflects the lack in restricting V_{pk} to non-negative values in the Cardarilli model.

As a final test, we perform an efficiency comparison simulating the same common-cathode stage in the WD domain employing both the proposed model and Cardarilli model. The two WD implementations, realized as GNU Octave scripts and available at <https://dangelo.audio/dafx2023-quadric.html>, differ only for the considered 3-port WD triode model. Under same operating conditions, we launch 20 runs of both algo-

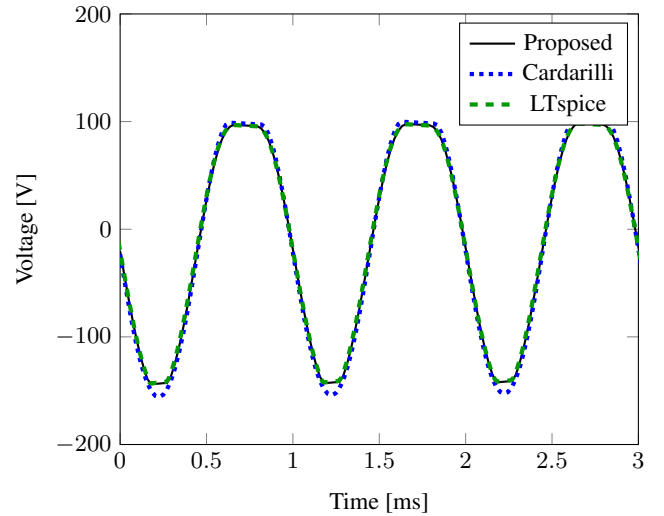


Figure 4: Voltage V_{out} at the output of the triode stage shown in Fig 3. The continuous black curve represents the result of the WD simulation employing the proposed model, the dotted blue curve represents the result of the WD simulation employing Cardarilli model, while the dashed green curve represents the LTspice simulation employing the proposed model.

gorithms on an AMD Ryzen 3 3200G processor, considering as input a mono guitar audio signal of duration 16 s and sampled at $f_s = 96$ kHz. We then measure the simulation time t_{sim} , and we average it over the number of runs for obtaining a fairer estimate. While the WD implementation with Cardarilli model takes on average 355.02 s, the WD implementation with the proposed model takes on average 76.55 s, showing thus a speedup of about $4.6\times$ over the traditional approach. It follows that the proposed quadric surface model is able to run much faster without compromising the accuracy of the representation, and, for this reason, can be a valuable triode model to be employed for real-time Virtual Analog applications.

5. CONCLUSIONS

In this paper, we proposed a novel triode model based on a quadric surface approximation. The model is characterized by only three parameters, involves simpler mathematical operations with respect to traditional models, such as Koren [21] and Cardarilli [22], and can lead to fully-explicit white box models. Considering the famous 12AX7 as a reference triode, we compared the plate current characteristics obtained with both the Cardarilli and Koren models and the proposed model to the one reported on its datasheet, showing that, when grid current is negligible, the new approach is more accurate than Koren’s and almost as accurate as Cardarilli’s even though the latter presents a number of parameters five times higher. Although the model can be realized in many circuit simulation methods, we decided to implement it as a 3-port WD block, which we later employed for the emulation of the typical common-cathode gain stage found in tube amplifiers. Under the same operating and modeling conditions, we drew an efficiency comparison between the quadric surface model and Cardarilli model, measur-

ing a $4.6\times$ speedup, which makes the proposed methodology very appealing for Virtual Analog applications.

Further work may concern the extension of the proposed model to other operating conditions by including, e.g., the tube diode between grid and cathode and the modeling of more complex vacuum tubes, such as tetrodes, pentodes, etc., by applying the same modeling methodology introduced in this paper but considering quadric hypersurfaces.

6. ACKNOWLEDGMENTS

S. D'Angelo would like to acknowledge Arturia for the time spent working on vacuum tube emulation back in 2015.

7. REFERENCES

- [1] Eero-Pekka Damskagg, Lauri Juvela, Etienne Thuillier, and Vesa Välimäki, "Deep Learning for Tube Amplifier Emulation," in *IEEE International Conference on Acoustics, Speech and Signal Processing (ICASSP)*, Brighton, UK, May 2019, pp. 471–475.
- [2] Damien Bouvier, Thomas Hélie, and David Roze, "Phase-based Order Separation for Volterra Series Identification," *International Journal of Control*, vol. 94, pp. 2104–2114, Aug. 2021.
- [3] Felix Eichas, Stephan Möller, and Udo Zölzer, "Block-Oriented Modeling of Distortion Audio Effects Using Iterative Minimization," in *Proceedings of the 18th International Conference on Digital Audio Effects (DAFx-15)*, Trondheim, Norway, Nov. 2015.
- [4] Antoine Falaize and Thomas Hélie, "Simulation of an Analog Circuit of a Wah Pedal: A Port-Hamiltonian Approach," in *Proceedings of the 135th Audio Engineering Society Convention*, Rome, Italy, May 2013, pp. 548–556.
- [5] Gianpaolo Borin, Giovanni De Poli, and Davide Rocchesso, "Elimination of Delay-Free Loops in Discrete-Time Models of Nonlinear Acoustic Systems," *IEEE Transactions on Speech and Audio Processing*, vol. 8, pp. 597–604, 2000.
- [6] Alfred Fettweis, "Wave Digital Filters: Theory and Practice," *Proceedings of the IEEE*, vol. 74, pp. 270–327, 1986.
- [7] Alberto Bernardini, Paolo Maffezzoni, and Augusto Sarti, "Linear Multistep Discretization Methods with Variable Step-Size in Nonlinear Wave Digital Structures for Virtual Analog Modeling," *IEEE/ACM Transactions on Audio, Speech, and Language Processing*, vol. 27, pp. 1763–1776, 2019.
- [8] Jyri Pakarinen and David T. Yeh, "A Review of Digital Techniques for Modeling Vacuum-tube Guitar Amplifiers," *Computer Music Journal*, vol. 33, pp. 85–100, 2009.
- [9] Karl Ralph Spangenberg, *Vacuum Tubes*, McGraw-Hill Book Company, 1948.
- [10] Thomaz Chaves de A. Oliveira, Gilmar Barreto, and Alexander Mattioli Pasqual, "Review of Digital Emulation of Vacuum-Tube Audio Amplifiers and Recent Advances in Related Virtual Analog Models," *INFOCOMP Journal of Computer Science*, vol. 12, pp. 10–23, 2015.
- [11] Udo Zölzer, *DAFX: Digital Audio Effects*, John Wiley and Sons, Ltd, Chichester, UK, Mar. 2011.
- [12] Kristjan Dempwolf and Udo Zölzer, "A Physically-motivated Triode Model for Circuit Simulations," in *Proceedings of the International Conference on Digital Audio Effects, DAFX*, Paris, France, 2011.
- [13] Ivan Cohen and Thomas Helie, "Measures and Parameter Estimation of Triodes, for the Real-Time Simulation of a Multi-Stage Guitar Preamplifier," in *129th Audio Engineering Society Convention 2010*, San Francisco, USA, 2010, vol. 1.
- [14] Giovanni De Sanctis and Augusto Sarti, "Virtual Analog Modeling in the Wave-Digital Domain," *IEEE Transactions on Audio, Speech, and Language Processing*, vol. 18, pp. 715–727, 2010.
- [15] Matti Karjalainen and Jyri Pakarinen, "Wave Digital Simulation of a Vacuum-Tube Amplifier," in *IEEE International Conference on Acoustics, Speech and Signal Processing (ICASSP)*, Toulouse, France, 2006, vol. 5.
- [16] Jaromir Mačák and Jiri Schimmel, "Real-Time Guitar Tube Amplifier Simulation using an Approximation of Differential Equations," in *13th International Conference on Digital Audio Effects (DAFx)*, Graz, Austria, Sept. 2010.
- [17] Jingjie Zhang and Julius O. Smith, "Real-time Wave Digital Simulation of Cascaded Vacuum Tube Amplifiers using Modified Blockwise Method," in *Proceedings of the International Conference on Digital Audio Effects (DAFx)*, Aveiro, Portugal, 2018, pp. 141–148.
- [18] Stefano D'Angelo, Jyri Pakarinen, and Vesa Välimäki, "New Family of Wave-Digital Triode Models," *IEEE Transactions on Audio, Speech, and Language Processing*, vol. 21, pp. 313–321, Feb. 2013.
- [19] W. Ross Dunkel, Maximilian Rest, Kurt James Werner, Michael Jørgen Olsen, and Julius O. Smith III, "The Fender Bassman 5F6-A Family of Preamplifier Circuits-A Wave Digital Filter Case Study," in *Proceedings of the International Conference on Digital Audio Effects (DAFx)*, Brno, Czech Republic, Sept. 2016.
- [20] Champ C. Darabundit, Dirk Roosenburg, and Julius O. Smith III, "Neural Net Tube Models for Wave Digital Filters," in *Proceedings of the 25th International Conference on Digital Audio Effects (DAFx)*, Vienna, Austria, Sept. 2022.
- [21] Norman L. Koren, "Improved Vacuum Tube Models for SPICE Simulations," *Glass Audio*, vol. 8, pp. 18–27, 1996.
- [22] Gian Carlo Cardarilli, Marco Re, and Leonardo Di Carlo, "Improved Large-Signal Model for Vacuum Triodes," in *Proceedings of the 2009 IEEE International Symposium on Circuits and Systems*, Taipei, Taiwan, May 2009.
- [23] Kenneth Levenberg, "A Method for the Solution of Certain Non-linear Problems in Least Squares," *Quarterly of Applied Mathematics*, vol. 2, 1944.
- [24] Jyri Pakarinen and Matti Karjalainen, "Enhanced Wave Digital Triode Model for Real-Time Tube Amplifier Emulation," *IEEE Transactions on Audio, Speech, and Language Processing*, vol. 18, pp. 738–746, 2010.
- [25] General Electric, "General Electric 12AX7 Electronic Tube - Datasheet," <http://www.r-type.org/pdfs/12ax7.pdf>.
- [26] Michèle Audin, *Geometry*, Springer Berlin Heidelberg, Berlin, Heidelberg, 2003.

- [27] Ivan Cohen and Thomas Hélie, “Measures and Models of Real Triodes, for the Simulation of Guitar Amplifiers,” *Acoustics 2012*, 2012.
- [28] Augusto Sarti and Giovanni De Sanctis, “Systematic Methods for the Implementation of Nonlinear Wave-Digital Structures,” *IEEE Transactions on Circuits and Systems I: Regular Papers*, vol. 56, pp. 460–472, 2009.
- [29] Kurt James Werner, Alberto Bernardini, Julius O. Smith, and Augusto Sarti, “Modeling Circuits with Arbitrary Topologies and Active Linear Multiports Using Wave Digital Filters,” *IEEE Transactions on Circuits and Systems I: Regular Papers*, vol. 65, pp. 4233–4246, 2018.
- [30] Alberto Bernardini, Paolo Maffezzoni, and Augusto Sarti, “Vector Wave Digital Filters and Their Application to Circuits With Two-Port Elements,” *IEEE Transactions on Circuits and Systems I: Regular Papers*, vol. 68, pp. 1269–1282, 2021.
- [31] Alberto Bernardini, Enrico Bozzo, Federico Fontana, and Augusto Sarti, “A Wave Digital Newton-Raphson Method for Virtual Analog Modeling of Audio Circuits with Multiple One-Port Nonlinearities,” *IEEE/ACM Transactions on Audio, Speech, and Language Processing*, vol. 29, pp. 2162 – 2173, 2021.
- [32] Alberto Bernardini, Kurt James Werner, Julius O. Smith, and Augusto Sarti, “Generalized Wave Digital Filter Realizations of Arbitrary Reciprocal Connection Networks,” *IEEE Transactions on Circuits and Systems I: Regular Papers*, vol. 66, pp. 694–707, 2019.
- [33] Alberto Bernardini, Alessio E. Vergani, and Augusto Sarti, “Wave Digital Modeling of Nonlinear 3-terminal Devices for Virtual Analog Applications,” *Circuits, Systems, and Signal Processing*, vol. 39, pp. 3289–3319, 2020.
- [34] Stefano D’Angelo and Vesa Välimäki, “Wave-Digital Polarity and current Inverters and their Application to Virtual Analao Audio Processing,” in *IEEE International Conference on Acoustics, Speech and Signal Processing (ICASSP)*, Vancouver, Canada, 2012.
- [35] Oliviero Massi, Riccardo Giampiccolo, Alberto Bernardini, and Augusto Sarti, “Explicit Vector Wave Digital Filter Modeling of Circuits with a Single Bipolar Junction Transistor,” in *Proceedings of the 26th International Conference on Digital Audio Effects (DAFx23)*, Copenhagen, Denmark, Sept. 2023.